Anal. Chem. **2000,** *72,* 4614−4622

Chiral Monolithic Columns for Enantioselective Capillary Electrochromatography Prepared by Copolymerization of a Monomer with Quinidine Functionality. 1. Optimization of Polymerization Conditions, Porous Properties, and Chemistry of the Stationary Phase

Michael Lämmerhofer, Eric C. Peters,† Cong Yu, Frantisek Svec, and Jean M. J. Fréchet*

Department of Chemistry, University of California, Berkeley, California 94720-1460

Wolfgang Lindner

Institute of Analytical Chemistry, University of Vienna, A-1090 Vienna, Austria

Monolithic columns for chiral capillary electrochromatography have been prepared within the confines of untreated fused-silica capillaries in a single step by a simple copolymerization of mixtures of *O*-[2-(methacryloyloxy)ethylcarbamoyl]-10,11-dihydroquinidine, ethylene dimethacrylate, and glycidyl methacrylate or 2-hydroxyethyl methacrylate in the presence of mixture of cyclohexanol and 1-dodecanol as a porogenic solvent. The porous properties of the monolithic columns can easily be controlled through changes in the composition of the binary porogenic solvent. Although both thermal- and UV light-initiated polymerizations afford useful capillary columns, monoliths prepared using the former approach exhibit better chromatographic properties. The ability to control pore size independently of the polymerization mixture composition enables the preparation of monoliths with varying percentages of the chiral monomer and cross-linker, as well as the optimization of their separation properties. Very good separations of model racemate (*R*,*S*)-*N*-3,5-dinitrobenzoylleucine were achieved using an optimized monolithic CEC column, with high efficiencies of up to 74 000 plates/m for the retained peaks.

The original promise of electrochromatography [1−3] to improve the efficiency of liquid chromatography by using an electrical field to achieve pluglike electroosmotic flow (EOF) for transporting analytes through a chromatographic column has materialized only recently.[4−6] Capillary electrochromatography (CEC) continues to develop rapidly and find applications in a variety of areas, including the separations of enantiomers.[7−23] Several groups have adapted an HPLC-like bead approach to a capillary column format in an attempt to achieve the high efficiencies predicted by theory. Although packed capillaries are currently the most common column technology, this approach is accompanied by several difficulties. For example, the surface charge often results only from residual surface silanols, making effective control of the magnitude and direction of EOF poor. Additionally, column packing procedures are often tedious, requiring in situ frit fabrication. These frits may have limited stability and/or permeability, and their heterogeneities may initiate spontaneous outgassing and bubble formation. These problems have led to the development of new column technologies—open-tubular and monolithic columns—that eliminate many of the drawbacks of packed capillary columns.

† Present address: Genomics Institute of the Novartis Research Foundation, San Diego, CA 92121-1125.

(1) Pretorius, V.; Hopkins, B. J.; Schieke, J. D. *J. Chromatogr.* **1974**, *99*, 23−30.
(2) Jorgenson, J. W.; Lukacs, K. D. *J. Chromatogr.* **1981**, *218*, 209−216.
(3) Knox, J. H.; Grant, I. H. *Chromatographia* **1987**, *24*, 135.
(4) Dittmann, M. M.; Rozing, G. P. *J. Chromatogr., A* **1996**, *744*, 63−74.
(5) Cikalo, M. G.; Bartle, K. D.; Robson, M. M.; Myers, P.; Euerby, M. R. *Analyst* **1998**, *123*, 87R−102R.
(6) Majors, R. E. *LC-GC* **1998**, *16*, 96−110.
(7) Schurig, V.; Wistuba, D. *Electrophoresis* **1999**, *20*, 2313−2328.
(8) Francotte, E.; Jung, M. *Chromatographia* **1996**, *42*, 521−527.
(9) Li, S.; Lloyd, D. K. *Anal. Chem.* **1993**, *65*, 3684−3690.
(10) Li, S.; Lloyd, D. K. *J. Chromatogr., A* **1994**, *666*, 321−335.
(11) Lelievre, F.; Yan, C.; Zare, R. N.; Gareil, P. *J. Chromatogr., A* **1996**, *723*, 145−156.
(12) Dermaux, A.; Lynen, F.; Sandra, P. *J. High Resolut. Chromatogr.* **1998**, *21*, 575−576.
(13) Carter-Finch, A. S.; Smith, N. W. *J. Chromatogr., A* **1999**, *848*, 375−385.
(14) Lämmerhofer, M.; Lindner, W. *J. Chromatogr., A* **1998**, *829*, 115−125.
(15) Tobler, E.; Lämmerhofer, M.; Lindner, W. *J. Chromatogr., A*, in press.
(16) Krause, K.; Chankvetadze, B.; Okamoto, Y.; Blaschke, G. *Electrophoresis* **1999**, *20*, 2272−2778.
(17) Krause, K.; Girod, M.; Chankvetadze, B.; Blaschke, G. *J. Chromatogr., A* **1999**, *837*, 51−63.
(18) Lin, J.-M.; Uchiyama, K.; Hobo, T. *Chromatographia* **1998**, *47*, 625−629.
(19) Schweitz, L.; Andersson, L. I.; Nilsson, S. *Anal. Chem.* **1997**, *69*, 1179−1183.
(20) Peters, E. C.; Lewandowski, K.; Petro, M.; Svec, F.; Fréchet, J. M. J. *Anal. Commun.* **1998**, *35*, 83−86.
(21) Koide, T.; Ueno, K. *Anal. Sci.* **1998**, *14*, 1021−1023.
(22) Wolf, C.; Spence, P. L.; Pirkle, W. H.; Derrico, E. M.; Cavender, D. M.; Rozing, G. P. *J. Chromatogr., A* **1997**, *782*, 175−179.
(23) Lämmerhofer, M.; Svec, F.; Fréchet, J. M. J.; Lindner, W. *Trends Anal. Chem.*, in press.

10.1021/ac000322l CCC: $19.00
Published on Web 09/02/2000

In open-tubular electrochromatography (OT-EC), the stationary phase is covalently attached, coated, or adsorbed onto the inner capillary wall.[24−26] Since the surface of the open tube is very limited, these columns only afford a low sample capacity. Selective etching of the wall may be used to increase the overall surface area and improve the loadability.[27] In contrast, monolithic stationary phases often possess much higher surface areas and adsorption capacities. To date, several different approaches to monolithic CEC columns have been reported: (i) Siliceous monoliths for CEC have been prepared by polycondensation of alkoxysilanes using a sol−gel process within the capillary tubing followed by postfunctionalization. [28] (ii) To minimize the risk of shrinkage typical of sol−gel transitions that can lead to cracks in the bed, the overall volume of the inorganic matrix was reduced by filling the column with traditional chromatographic particles prior to initiating the sol−gel process.[29−32] (iii) Consolidation of a packed bed by sintering the particles has also been proposed as a method for the preparation of monolithic columns, but this technique is even more laborious and the surface chemistry of the stationary phase is often destroyed during the sintering process necessitating postfunctionalization. [33,34] (iv) Functional monomers have been polymerized in situ within bare or vinylized fused-silica tubing in the presence of pore-forming solvents to yield continuous porous cross-linked organic polymers.[35] Examples of this approach include polyacrylamide-based gels,[36−40] polyacrylamide copolymers prepared in the presence of poly(ethylene glycol),[41] molecularly imprinted "superporous" monoliths,[19,42] and highly cross-linked polystyrene[43,44] and polymethacrylate matrixes.[45−49] However, only a few studies have attempted the use of monolith technology for enantiomeric separations.[19,20,42,50,51]

Recently, we described the preparation of chiral monolithic CEC columns by a single-step copolymerization process.[20] This approach required the simultaneous incorporation of both a valine-derived selector monomer and a negatively charged monomer (2-acrylamido-2-methyl-1-propanesulfonic acid) into the monolithic structure. We now report a vastly simplified copolymerization technique using a polymerizable quinidine carbamate that combines (i) an ionizable strongly basic quinuclidine functionality with (ii) multiple interaction sites (cationic quinuclidine, carbamate, and quinoline) suitably located within a semirigid molecular framework. These interactions sites contain both stereogenic centers and bulky groups to form series of favorable binding pockets.[52−54] The quinidine functionality plays a double role, providing the surface charges required to generate EOF and therefore eliminating the need for the addition of a charged comonomer, as well as affording the required stereoselective interactions to complementary chiral analytes, resulting in the separation of enantiomers. In this paper, we discuss the preparation method, chemistry, and morphology of the stationary phase for chiral CEC.

EXPERIMENTAL SECTION

Materials. 10,11-Dihydroquinidine base and 1-dodecanol were purchased from Fluka. 2-Isocyanatoethyl methacrylate was from the Dow Chemical Co. (Midland, MI). Azobisisobutyronitrile (AIBN), dibutyltin dilaurate, 4-methoxyphenol, and cyclohexanol were obtained from Aldrich. Ethylene dimethacrylate (EDMA) and glycidyl methacrylate (GMA) were from Sartomer (West Chester, PA), and 2-hydroxyethyl methacrylate (HEMA) was from Kodak (Rochester, NY). Racemic *N*-3,5-dinitrobenzoylleucine (DNB-Leu) as well as its *S*-enantiomer were purchased from Aldrich. The preparation of *N*-3,5-dinitrobenzyloxycarbonylleucine (DNZ-Leu) has been described elsewhere.[55]

Caution: Several methacrylates and solvents are known sensitizing agents. Proper precautions should be taken during the physical handling of these materials.

Fused-silica capillaries (100 μm i.d.) with both conventional polyimide and UV-transparent fluorinated hydrocarbon polymer coatings were obtained from Polymicro Technologies (Phoenix, AZ).

***O*-[2-(Methacryloyloxy)ethylcarbamoyl]-10,11-dihydroquinidine (1).** 10,11-Dihydroquinidine and 2-isocyanatoethyl methacrylate (1.1 molar excess) were dissolved in dry THF. After the addition of 3 drops of a catalyst (dibutyltin dilaurate) and 100 μL of an inhibitor solution (4-methoxyphenol, 1 mg/mL in dry THF), the reaction mixture was stirred overnight at room temperature. The solvent was evaporated and the residue purified by flash chromatography on silica using a chloroform/methanol

(24) Tsuda, T.; Nomura, K.; Nakagawa, G. *J. Chromatogr.* **1982**, *248*, 241−247.
(25) Guo, Y.; Colon, L. A. *Anal. Chem.* **1995**, *67*, 2511−2516.
(26) Sawada, H.; Jinno, K. *Electrophoresis* **1999**, *20*, 24−30.
(27) Pesek, J. J.; Matyska, M. T. *J. Chromatogr., A* **1996**, *736*, 255.
(28) Tanaka, N.; Nagayama, H.; Kobayashi, H.; Ikegami, T.; Hosoya, K.; Ishizuka, N.; Minakuchi, H.; Nakanishi, K.; Cabrera, K.; Lubda, D. *J. High Resolut. Chromatogr.* **2000**, *23*, 111−116.
(29) Dulay, M. T.; Kulkarni, R. P.; Zare, R. N. *Anal. Chem.* **1998**, *70*, 5103−5107.
(30) Tang, Q. L.; Xin, B. M.; Lee, M. L. *J. Chromatogr., A* **1999**, *837*, 35−50.
(31) Chirica, G.; Remcho, V. T. *Electrophoresis* **1999**, *20*, 50−56.
(32) Ratnayake, C. K.; Oh, C. S.; Henry, M. P. *J. High Resolut. Chromatogr.* **2000**, *23*, 81−88.
(33) Dittmann, M. M.; Rozing, G. P.; Ross, G.; Adam, T.; Unger, K. K. *J. Capillary Electrophoresis* **1997**, *4*, 201−212.
(34) Asiaie, R.; Huang, X.; Farnan, D.; Horváth, C. *J. Chromatogr., A* **1998**, *806*, 251−263.
(35) Svec, F.; Peters, E. C.; Sýkora, D.; Cong Yu, J.; Fréchet, M. J. *J. High Resolut. Chromatogr.* **2000**, *23*, 3−18.
(36) Liao, J.-L.; Chen, N.; Ericson, C.; Hjerten, S. *Anal. Chem.* **1996**, *68*, 3468−3472.
(37) Ericson, C.; Hjerten, S. *Anal. Chem.* **1999**, *71*, 1621−1627.
(38) Hjertén, S. *Ind. Eng. Chem. Res.* **1999**, *38*, 1205−1214.
(39) Fujimoto, C.; Kino, J.; Sawada, H. *J. Chromatogr., A* **1995**, *716*, 107−113.
(40) Fujimoto, C.; Fujise, Y.; Matsuzawa, E. *Anal. Chem.* **1996**, *68*, 2753−2757.
(41) Palm, A.; Novotny, M. V. *Anal. Chem.* **1997**, *69*, 4499−4507. Que, A. H.; Konse, T.; Baker, A. G.; Novotny, M. V. *Anal. Chem.* **2000**, *72*, 2703−2710.
(42) Nilsson, K.; Lindell, J.; Norrlöw, O.; Sellergren, B. *J. Chromatogr., A* **1994**, *680*, 57−61. Schweitz, L.; Andersson, L. I.; Nilsson, S. *J. Chromatogr., A* **1998**, *817*, 5−13.
(43) Gusev, I.; Huang, X.; Horváth, C. *J. Chromatogr., A* **1999**, *855*, 273−290.
(44) Xiong, B.; Zhang, L.; Zhang, Y.; Zou, H.; Wang, J. *J. High Resolut. Chromatogr.* **2000**, *23*, 67−72.
(45) Peters, E. C.; Petro, M.; Svec, F.; Fréchet, J. M. J. *Anal. Chem.* **1997**, *69*, 3646−3649.
(46) Peters, E. C.; Petro, M.; Svec, F.; Fréchet, J. M. J. *Anal. Chem.* **1998**, *70*, 2288−2295.
(47) Peters, E. C.; Petro, M.; Svec, F.; Fréchet, J. M. J. *Anal. Chem.* **1998**, *70*, 2296−2302.
(48) Svec, F.; Fréchet, J. M. J. *Ind. Eng. Chem. Res.* **1999**, *38*, 34−38.
(49) Yu, C.; Svec, F.; Fréchet, J. M. J. *Electrophoresis* **2000**, *21*, 120−127.
(50) Koide, T.; Ueno, K. *Anal. Sci.* **1999**, *15*, 791−794.
(51) Koide, T.; Ueno, K. *J. High Resolut. Chromatogr.* **2000**, *23*, 59−66.
(52) Lämmerhofer, M.; Lindner, W. *J. Chromatogr., A* **1996**, *741*, 33−48.
(53) Maier, N. M.; Nicoletti, L.; Lämmerhofer, M.; Lindner, W. *Chirality* **1999**, *11*, 522−528.
(54) Schefzick, S.; Lindner, W.; Lipkowitz, K. B. *Chirality* **2000**, *12*, 7−15.
(55) Piette, V.; Lämmerhofer, M.; Bischoff, K.; Lindner, W. *Chirality* **1997**, *9*, 157−161.

mixture as the eluent. The product was recrystallized from dichloromethane/petroleum ether. Physical properties: mp 109−111 °C; $[\alpha]^{23}_{Na589} = +62.0$, $[\alpha]^{23}_{Hg578} = +65.2$, $[\alpha]^{23}_{Hg546} = +73.7$ ($c = 0.988$; MeOH); IR (KBr) 3420, 3200, 2920, 2870, 1715, 1620, 1570, 1530, 1500 cm^{-1}; ^1H NMR ($CDCl_3$) δ 0.93 (t, 3H), 1.2−1.85 (m, 8H), 1.90 (s, 3H), 2.55−2.95 (m, 4H), 3.24 (m, 1H), 3.50 (m, 2H), 3.98 (s, 3H), 4.2 (t, 2H), 5.10 (s, 1H), 5.50 (s, 1H), 6.03 (s, 1H), 6.48 (d, 1H), 7.36 (m, 2H), 7.46 (d, 1H), 8.00 (d, 1H), 8.75 (d, 1H) ppm.

Preparation of the Monolithic Capillary Columns. Free-radical initiator (AIBN, 1 wt % with respect to the monomers) was added to a polymerization mixture consisting of 40 wt % monomers (**1** + comonomer (GMA or HEMA) + cross-linker (EDMA) in various proportions) and 60 wt % porogenic solvent mixture of 1-dodecanol and cyclohexanol. The container with reaction mixture was placed in an ice/water bath, sonicated for 10 min to obtain a clear solution, and then purged with nitrogen for 10 min. Using a 100-μL syringe and a short Teflon sleeve, this polymerization mixture was transferred into 50-cm-long capillaries, filling a 35-cm-long segment, and the capillaries were then sealed at both ends with rubber stoppers.

Polyimide-coated capillaries were used for thermally initiated polymerization. The filled capillaries and a sealed glass vial containing the remaining polymerization mixture were submerged into a water bath and allowed to react for 20 h at 60 °C. UV-initiated polymerization was carried out in capillaries having a fluorinated hydrocarbon coating. In contrast to glass vials used in the thermal process, the remainder of the polymerization mixture was polymerized in a quartz glass tube sealed with a Teflon film. Capillaries and the tube were placed in a box equipped with two 8-W UV lamps (VWR Scientific Products) and irradiated at room temperature for 16 h.

The bulk polymers were crushed to small pieces, Soxhlet-extracted with methanol for 12 h, and vacuum-dried at 60 °C. These polymers were used for the porosimetric measurements and elemental analysis. The monolithic capillaries were washed directly with the mobile phase (acetonitrile/methanol 80:20 containing 0.4 mol/L acetic acid and 4 mmol/L triethylamine) to remove unreacted monomers and porogens using a micropump (model 260D, Isco, Lincoln, NE). Typically, back pressures of 14−20 MPa (2000−3000 psi) were generated at flow rates of 1−3 μL/min. All of the tested columns tolerated these high pressures without extrusion or visible compression of the polymer monolith. The capillaries were then cut at both ends to a total length of 33.5 cm and a bed length of 25 cm, leaving a 8.5cm-long open segment between the detection window and the outlet end. Capillaries with the UV-transparent coating were placed in the alignment interface of the cassette, while a detection window was first created on polyimide-coated capillaries at the end of the continuous bed using a razor blade.

Characterization of Porous Properties. The pore size distributions of the porous monolithic materials were determined using an Autopore III 9400 mercury intrusion porosimeter (Micromeritics, Norcross, GA). Specific surface areas were measured by nitrogen adsorption/desorption (ASAP 2010, Micromeritics) and calculated using the BET equation. Scanning electron microscopy (SEM) images were obtained using a JEOL JSM6300 electron microscope.

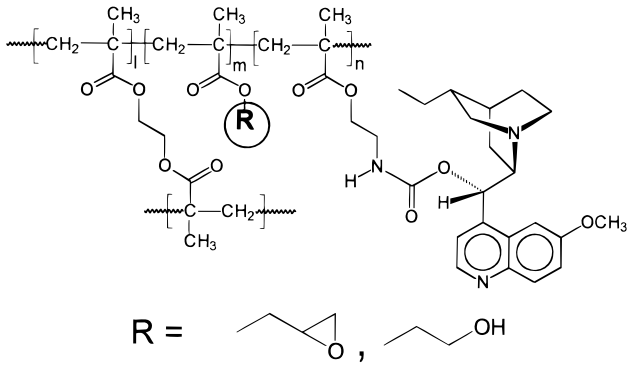

Figure 1. Simplified chemical structure of the chiral monolithic polymer prepared by copolymerization of quinidine-functionalized chiral monomer **1**, ethylene dimethacrylate, and glycidyl methacrylate or 2-hydroxyethyl methacrylate.

CEC Experiments. CEC experiments were carried out using a modified $HP^{3D}CE$ capillary electrophoresis instrument (Hewlett-Packard, Palo Alto, CA) equipped with a diode array detector and an external pressurization system. An equal pressure of 0.6 MPa (87 psi) was applied at both ends of the capillary column. The mobile phase consisted of acetonitrile/methanol (80:20 v/v), containing 0.4 mol/L acetic acid and 4 mmol/L triethylamine as electrolytes. The sample solutions (0.5 mg/mL) were injected electrokinetically (−15 kV for 5 s) and the separations performed at a voltage of −25 kV and at a temperature of 50 °C. The peaks were monitored at a wavelength of 250 nm and processed by the HP ChemStation software. Acetone was added as an EOF marker.

RESULTS AND DISCUSSION

Preparation of Monolithic Columns. The major advantage of our procedure is its simplicity for the straightforward preparation of the monolithic media. No pretreatment of the capillary wall and/or postfunctionalization of the monolithic column is required. The monoliths are prepared directly within fused-silica tubing by in situ copolymerization of quinidine-based chiral monomer **1**, which is readily accessible in very high yields using a single-step synthesis. The quinidine functionalities are directly incorporated into the porous polymer (Figure 1) together with a suitable comonomer and substantial amounts of cross-linker in the presence of a porogenic solvent. The polymerization is initiated either by heating or by UV irradiation. The chemical composition of the polymer is easily controlled by varying the percentages of the various monomers in the reaction mixture, allowing the properties of the monolithic column to easily be tailored for the desired chromatographic application. For example, changes in the ratio of comonomer to chiral monomer **1** determine the degree of functionalization of the monolith. The surface-exposed quinidine carbamate moieties that are positively charged under the CEC conditions employed provide specific interaction sites for chiral analytes. Because they are charged, these groups also generate the EOF. While a relatively modest number of cationic quinidine groups might be sufficient to achieve high EOF rates, high levels of functionalization of the chiral moieties are desirable for effective chiral discrimination. Selector contents in excess of 0.2 mmol/g of polymer, corresponding to more than 10 wt % of the total monomers, are required to achieve good separation of target analytes.

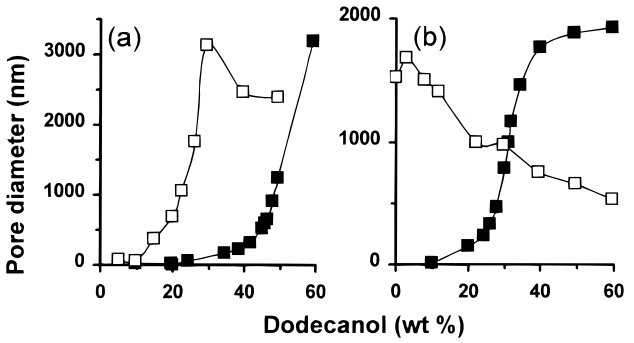

Figure 2. Effect of thermal (a) and UV initiation (b), type of comonomer, and percentage of 1-dodecanol in the polymerization mixture on the mode pore diameter of quinidine-functionalized chiral monoliths. Reaction conditions: polymerization mixture, chiral monomer 8 wt %, glycidyl methacrylate (□) or 2-hydroxyethyl methacrylate (■) 16 wt %, ethylene dimethacrylate 16 wt %, and porogenic solvent 60 wt % (consisting of 1-dodecanol and cyclohexanol) ; polymerization time, 20 h at 60 °C (a) and 16 h at room temperature (b).

Table 1. Physical Properties of Quinidine-Functionalized Chiral Monoliths[a]

dodecanol (wt %)	V_p[b] (mL/g)	$d_{p,mode}$[c] (nm)	S[d] (m^2/g)	selector[e] (mmol/g)	current[f,g] (μA)	u[f] (mm/s)
			UV Initiation			
39.8	1.20	1770	<1	0.40	−7.6	1.45
34.6	1.03	1463	1.0	0.40	−6.4	1.31
32.0	1.18	1163	3.5	0.42	−7.2	1.34
31.2	0.87	952	2.9	0.42	−6.4	1.70
30.0	0.96	782	3.7	0.40	−5.4	1.40
29.1	1.01	698	8.3	0.36	−5.9	1.04
27.1	0.80	465	5.4	0.35	−2.8	1.13
26.2	1.01	333	8.3	0.38	−2.8	0.74
			Thermal Initiation			
59.5	1.33	3166	<1	0.36	−10.9	1.41
49.4	1.19	1232	5.1	0.40	−5.9	1.23
49.2	1.17	1064	7.9	0.45	−5.5	1.08
47.6	1.36	824	6.3	0.41	−6.2	0.95
46.9	1.23	782	6.0	0.39	−5.8	0.88
46.5	1.26	651	7.8	0.40	−4.1	0.95
46.0	1.35	589	9.4	0.41	−3.9	0.89
45.1	1.23	510	13.5	0.39	−2.2	0.64

[a] Composition of polymerization mixture: 8 wt % **1**, 16 wt % HEMA, 16 wt % EDMA, and dodecanol + cyclohexanol 60 wt %. [b] Pore volume. [c] Pore diameter at maximum of the distribution curve. [d] BET surface area. [e] Quinidine selector moieties incorporated into monolith according to elemental analysis of nitrogen. [f] For CEC standard conditions, mobile phase 0.4 mol/L acetic acid and 4 mmol/L triethylamine in acetonitrile/methanol (80:20, v/v), voltage − 25 kV, and capillary temperature 50 °C. [g] Current in untreated open fused-silica capillary at +25 kV is +28 mA.

The monovinyl comonomer provides the surface functionalities that contribute to the chromatographic separations. On that basis of our previous experience,[20] GMA and HEMA were used to control the polarity of the pore surface. In contrast, in our earlier work, we had developed polymerization conditions for both thermally initiated[46] and photoinitiated systems[49] that afforded hydrophobic butyl methacrylate-based monoliths suitable for reversed-phase CEC applications. Therefore, the polymerization conditions had to be reoptimized with the new polymerization mixture to obtain monoliths suited for chiral CEC.

In sharp contrast to other approaches that may require covalent bonding of the monolith to the capillary wall to avoid extrusion of the matrix, no pretreatment of the capillary is required while working with monoliths.[45−47,49] In addition, the electrostatic forces between the basic quinuclidine functionalities of the monolith and the acidic surface silanol groups of the fused-silica capillary typical of our present approach also contribute to the attraction and exclude the undesired dislodging of the monolith. The monolithic capillary columns easily withstood pressures of up to 28 MPa (4000 psi) that were applied during the initial washing step with a pressurized flow driven by a mechanical pump. In addition, numerous changes in both the mobile-phase composition and the strength of the electrical field during CEC applications did not decrease the adhesion of the monolith to the wall.

Effect of Porogen Composition on Porous Properties. It is very important to finely tune the pore structure of the monolithic stationary phase, since the monolith operation must be in a flow-through mode. A number of variables are available to control the porous properties of macroporous materials, including the percentage of cross-linker, reaction temperature, concentration of initiator, and composition and percentage of the porogenic solvent. A binary porogenic solvent consisting of cyclohexanol and 1-dodecanol enables the fine control of the porous structure in systems containing **1**, EDMA, and GMA or HEMA.

Figure 2 shows the effect of dodecanol content in the porogenic solvent mixture on mode pore size (pore diameter at the maximum of the distribution curve) for monoliths prepared from mixtures containing GMA or HEMA as a comonomer using either thermal or UV initiations. Both the nature of the comonomer and the initiation method affect the porous structure. Compared to GMA-containing monoliths, a much higher content of dodecanol in the dodecanol/cyclohexanol mixture is generally required to obtain HEMA-containing monoliths with sufficiently large pores. For example, GMA monoliths with a mode pore size of 1000 nm are obtained by thermal polymerization at 60 °C using a polymerization mixture containing 20% dodecanol and 40% cyclohexanol. In contrast, a much higher percentage of the less polar dodecanol (50%) is required for the preparation of HEMA-containing monoliths with a similar pore size (Figure 2a).

Photoinitiated polymerization of the same mixtures at 20 °C generally yields monoliths with larger pores compared to those initiated thermally. Thus, the dodecanol content in the polymerization mixture used for UV-initiated polymerizations has to be reduced in order to obtain pore sizes comparable to those of their thermally polymerized analogues. For example, a polymerization mixture containing only 30% dodecanol produces a monolith with 1000-nm pores by UV polymerization when HEMA is used as the comonomer. These shifts can readily be explained by the effect of the polymerization temperature, since the creation of larger pores is favored at lower temperatures.[56]

The physical properties of quinidine-functionalized HEMA monoliths prepared by both UV and thermally initiated polymerizations are summarized in Table 1 and indicate that good control of the mode pore size can be exerted over a rather broad range. As expected, the specific surface areas ranging from 1 to 15 m^2/g are inversely proportional to the pore size. It should be noted that the SEM images (not shown) of the morphologies of both UV and thermally polymerized monoliths prepared from the same monomer mixture but with porogens having adjusted composi-

(56) Svec, F.; Fréchet, J. M. J. *Macromolecules* **1995**, *28*, 7580−7582.

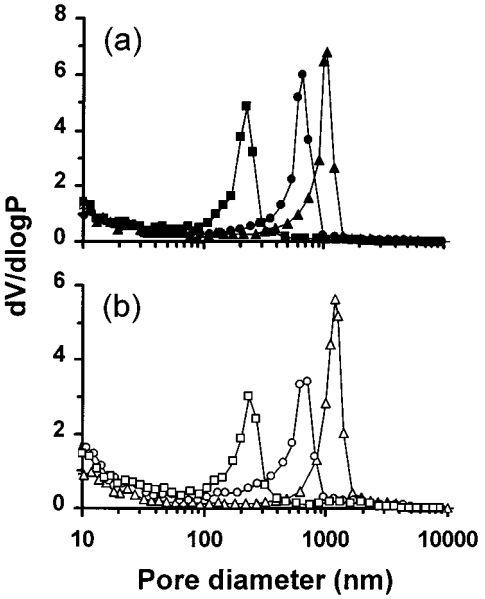

Figure 3. Differential pore size distribution profiles of poly(**1**-*co*-hydroxyethyl methacrylate-*co*-ethylene dimethacrylate) monoliths prepared using thermal (a) and UV-initiated polymerization (b). Reaction conditions: polymerization mixture, chiral monomer 8 wt %, 2-hydroxyethyl methacrylate 16 wt %, ethylene dimethacrylate 16 wt %, and porogenic solvent 60 wt % (consisting of 39 (■), 47 (●), 50 (▲), 25 (□), 29 (○), and 32 (△) wt % 1-dodecanol and cyclohexanol); thermal polymerization 20 h at 60 °C and UV polymerization 16 h at room temperature.

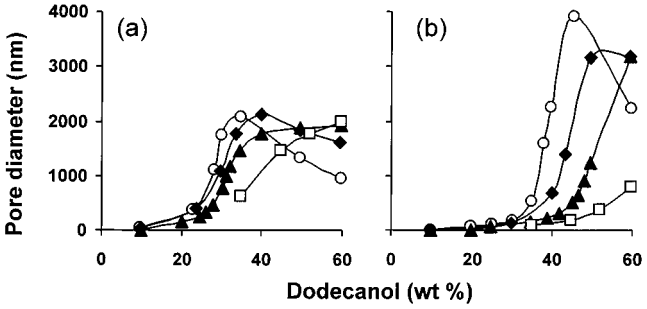

Figure 4. Effect of percentage of chiral monomer **1** and 1-dodecanol on pore size of the monoliths prepared using UV- (a) and thermal-initiated polymerization (b). Reaction conditions: polymerization mixture, chiral monomer 0 (○), 4 (♦), 8 (▲), and 12 wt % (□), 2-hydroxyethyl methacrylate 24-[percentage of **1**] wt %, ethylene dimethacrylate 16 wt %, and porogenic solvent 60 wt % (consisting of 1-dodecanol and cyclohexanol); polymerization time 16 h at room temperature (a) and 20 h at 60 °C (b).

tions that lead to equal modal pore diameter do not reveal any significant differences. This is also confirmed by the very similar pore size distribution profiles shown in Figure 3. The curves are unimodal with one distinct maximum in the macropore range regardless of the preparation procedure.

Content of Chiral Monomer. The porous properties of the monoliths also depend on the percentage of chiral monomer **1** in the polymerization mixture. Changes in the chemical composition of a polymer chain affect its solubility and therefore control the onset of phase separation during the polymerization process. As shown in Figure 4 for both photoinitiated and thermally initiated polymerizations, an increase in the percentage of **1** in the polymerization mixture at a fixed composition of porogen leads to a significant decrease in the pore size. For example, a photopolymerized monolith with a mode pore diameter of 1600 nm is obtained using a mixture consisting of 4% **1** and 20% HEMA, in addition to 16% EDMA, 35% 1-dodecanol, and 25% cyclohexanol. Monoliths with smaller pore diameters of 1400 and 600 nm are obtained, if the percentage of **1** is increased to 8 and 12%, respectively, with a concomitant decrease in HEMA (Figure 4a). A further increase in the percentage of **1**, while using the same porogen mixture, affords monoliths with no macroporosity. An increase in dodecanol content makes macroporous structures accessible even at higher percentages of monomer **1** using UV-initiated polymerization. Pure dodecanol as a porogen affords monoliths with a pore size of 1300 nm from a polymerization mixture containing 16% **1**. However, even pure dodecanol does not produce sufficiently large pores from mixtures containing 24% **1**. Therefore, a completely different porogen system would have to be developed. Although the thermally initiated system behaves slightly differently, the overall effects are very similar as shown in Figure 4b.

Effect of the Amount of Chiral Monomer on the Chromatographic Properties. The simplicity of this monolithic technology enables the easy preparation of capillary columns with varying contents of the chiral monomer. Its level of incorporation into the monolith affects flow rates (both pressurized and electroosmotic), adsorption capacity, retention, and enantioselectivity, thus largely determining the chromatographic properties of these separation media.

The effects of increasing the percentage of chiral monomer in the UV-initiated polymerization on the physical and chromatographic properties of the resulting monoliths with pore sizes adjusted to two different values are illustrated in Table 2. Increases in the percentage of chiral monomer were compensated by reductions in HEMA level, while the percentage of cross-linking monomer was held constant. Various compositions of the porogenic mixture specified in Table 2 were used to obtain monoliths with comparable pore sizes. Since the chiral monomer is almost completely incorporated, its loading corresponds to the initial percentage of **1** in the monomer mixture. For example, monoliths with 0.2 and 0.6 mmol/g selector as measured by elemental analysis are obtained by photopolymerization of a mixture containing 4 and 12 wt % of the chiral monomer.

Since the chiral monomer also provides the driving force for EOF, an increase in its loading should result in an increase in the electroosmotic flow velocity. Surprisingly, this effect is not very dramatic. Only a minor increase in flow velocity from 0.97 to 1.12 mm/s is observed for monoliths with the lower mode pore diameter as the loading with monomer **1** triples. Velocity fluctuations of similar magnitude were also found for the larger pore size monoliths. No flow could be achieved with the monolith prepared from polymerization mixture containing 16% **1** (40% of total monomers).

In contrast, the loading of **1** has a much larger effect on retention. As seen in Table 2, a 5-fold increase in the effective retention factor of both enantiomers is observed as the overall loading increases from 0.21 to 0.64 mmol/g. This indicates that the level of surface coverage of quinidine functionalities also increases. Interestingly, there is almost no effect of loading on the selectivity factor α. Taking into account the small effects of increased loading on both flow velocity and selectivity, it might

Table 2. Physical and Chromatographic Properties of Quinidine-Functionalized Chiral Monoliths with Different Selector Content

polym mixt, (wt %)		dodecanol	V_p[b]	$d_{p,mode}$[c]	S[d]	selector[e]	current[f,g]	u[f]	DNZ-Leu					
1	HEMA	(wt %)	(mL/g)	(nm)	(m^2/g)	(mmol/g)	(μA)	(mm/s)	$k_{eff}(S)$	$k_{eff}(R)$	α	R_S	$N_{(S)}$ (m^{-1})	$N_{(R)}$ (m^{-1})
4	20	27.1	0.98	865	3.3	0.21	−11.4	0.97	0.91	1.11	1.22	1.30	5504	4389
8	16	29.1	1.01	698	8.3	0.36	−5.9	1.04	2.73	3.66	1.34	2.29	6748	6100
12	12	34.9	0.94	621	6.9	0.64	−5.2	1.12	4.37	5.55	1.27	3.04	15374	13085
4	20	49.5	0.97	1836	1.3	0.21	−9.6	1.34	0.72	0.72	*h*	0.00	102	102
8	16	39.8	1.20	1770	<1	0.04	−7.6	1.45	2.39	3.21	1.35	1.21	1996	1726
12	12	51.8	1.04	1758	<1	0.61	−5.7	1.19	3.85	5.30	1.38	2.92	8133	7081
16	8	59.6	0.86	1322	1.0	0.79	*i*	*i*						

[a] The mixture also contains 16 wt % EDMA and 60 wt % porogens (consisting of cyclohexanol and dodecanol); UV-initiated polymerization 16 h at room temperature. [b] Pore volume. [c] Pore diameter at maximum of the distribution curve. [d] BET surface area. [e] Quinidine selector moieties incorporated into monolith according to elemental analysis of nitrogen. [f] For CEC standard conditions, mobile phase 0.4 mol/L acetic acid and 4 mmol/L triethylamine in acetonitrile/methanol (80:20, v/v), voltage −25 kV, and capillary temperature 50 °C. [g] Current in untreated open fused-silica capillary at +25 kV is +28 μA. [h] Selectivity factor cannot be determined correctly, since the peak shapes do not enable precise reading of the retention times. [i] No electroosmotic flow was observed for this monolithic column.

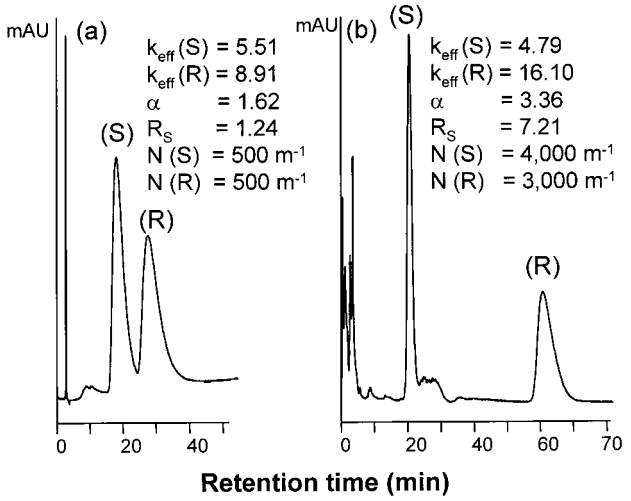

Figure 5. Electrochromatographic performance of monoliths with glycidyl methacrylate (a) and 2-hydroxyethyl methacrylate (b) as comonomers. Conditions: capillary column 335 mm (250-mm active length) × 0.1 mm i.d., pore size 993 (a) and 1163 nm (b); analyte DNB-(*R*,*S*)-leucine; mobile phase, 400 mM acetic acid and 4 mM triethylamine in acetonitrile/methanol (80:20, v/v); voltage, −25 kV; temperature, 30 °C.

appear that a high content of **1** in the monoliths is not desirable, as its only effect appears to be an increase in the retention time.

However, the loading level has a significant effect on column efficiency (Table 2). Monoliths of both small and large pore sizes with higher quinidine content exhibit much higher efficiencies. Considering all the effects, a selector loading of 0.4 mmol/g represents an optimum that affords monolithic columns with reasonably long retentions, good selectivities, and good efficiencies.

Effect of Comonomer. Figure 5 shows the effect of comonomer polarity on the CEC separation of DNB-leucine enantiomers using monoliths prepared from the quinidine-functionalized chiral monomer and glycidyl methacrylate or 2-hydroxyethyl methacrylate. The polarity of the surface clearly affects both the enantioselectivity and the efficiency of a monolithic capillary column. We observed a similar positive effect of a more hydrophilic polymer matrix on enantiomeric separations in our earlier study that investigated monolithic capillary columns prepared from polymerization mixtures containing an amino acid-based chiral monomer. The substitution of glycidyl methacrylate for butyl methacrylate, and the subsequent hydrolysis of the epoxide groups to vicinal diol moieties, considerably improved the column efficiency.[20] In this study, the simple replacement of GMA with the more polar HEMA increases the column efficiency of these nonoptimized capillaries by a factor of 8 from 500 to 4000 theoretical plates/m. Simultaneously, the enantioselectivity for DNB-Leu rapidly increases from an α factor of 1.62 to 3.36. This effect can be attributed to the significant reduction of nonspecific interactions, as well as the absence of lateral epoxypropyl functionalities with uncontrolled stereochemistry at the central carbon atom. Although the epoxide groups can be hydrolyzed in situ to obtain more polar diol functionalities, this represents an additional reaction step that complicates the preparation procedure and does not address the detrimental effect of the uncontrolled chirality. Since the improvement achieved by substituting HEMA for GMA was substantial, our further studies were carried out only with poly(**1**-*co*-HEMA-*co*-EDMA) monoliths.

Effect of Initiation. Monoliths prepared by thermally initiated polymerization always gave higher enantioselectivities than their counterparts prepared by UV-initiated polymerization. Interestingly, only small variations in selectivity factors α are observed across a broad range of pore sizes. Figure 3 shows that the pore size distribution profiles of poly(**1**-*co*-HEMA-*co*-EDMA) monoliths having equal mode pore sizes as determined by mercury intrusion porosimetry are similar regardless of the initiation process employed. Table 1 indicates that the thermally polymerized monoliths consistently possess surface areas almost twice as large as those polymerized using UV initiation. Since mercury porosimetry measurements afford identical profiles in the pore size range of 10−10 000 nm, this difference has to arise from differences in the small mesopores (2−10 nm) and micropores (<2 nm). Two factors might be responsible for the better selectivity of the thermally polymerized monoliths. The first is surface area, since a larger surface should translate into higher selectivity as a result of the larger number of exposed interacting groups. This factor may however be excluded since experiments shown in Table 2 that involve monolith with various loadings of chiral

Table 3. Effect of Cross-Linking on the Physical Properties of Quinidine-Functionalized Chiral Monoliths Prepared by UV-Initiated Polymerization

polymerization mixture, wt %[a]		V_p[b]	$d_{p,mode}$[c]	S[d]	selector[e]	current[f,g]	u[f]
EDMA	HEMA	(ml/g)	(nm)	(m^2/g)	(mmol/g)	(μA)	(mm/s)
16	16	1.01	698	8.3	0.36	−5.9	1.04
12	20	0.89	616	2.6	0.41	−3.6	0.72
8	24	0.75	1046	1.4	0.42	−3.8	0.85
4	28	0.23	1097	< 1	0.37	−5.1	0.52
2	30	0.00	nonmacroporous monolith			-[h]	-[h]

[a] The mixture also contains 8 wt % 1, 30 wt % cyclohexanol, and 30 wt % dodecanol. [b] Pore volume. [c] Pore diameter at maximum of the distribution curve. [d] BET surface area. [e] Quinidine selector moieties incorporated into monolith according to elemental analysis of nitrogen. [f] For CEC standard conditions mobile phase 0.4 mol/L acetic acid and 4 mmol/L triethylamine in acetonitrile-methanol (80:20, v/v), voltage − 25 kV, capillary temperature 50 °C. [g] Current in untreated open fused silica capillary at +25 kV is +28 mA. [h] No electroosmotic flow was observed for this monolithic column.

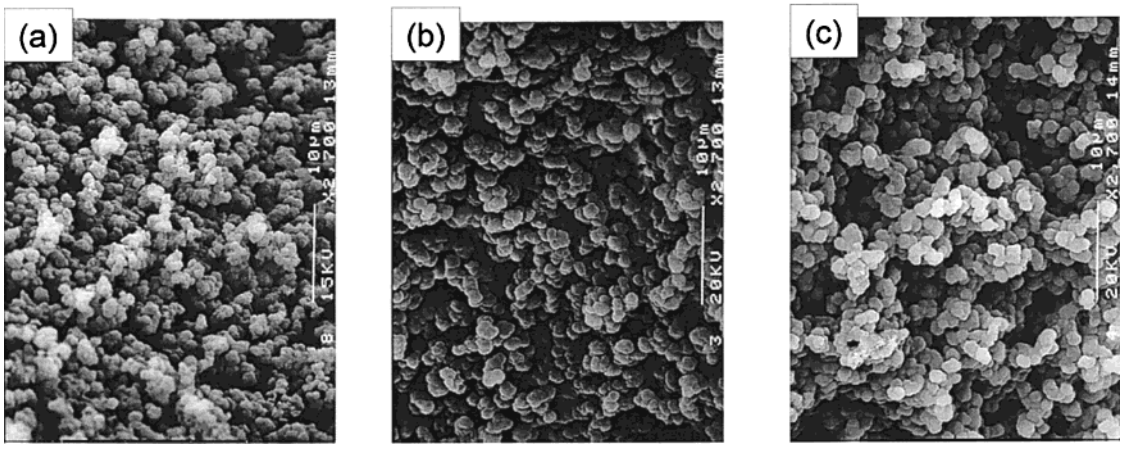

Figure 6. Scanning electron micrographs of quinidine-functionalized monoliths with different cross-linking levels prepared by UV-initiated polymerization. Polymerization mixture. total monomers 40 wt % (consisting of chiral monomer 8 wt %, ethylene dimethacrylate 16 (a), 8 (b), and 4 wt % (c), complementary percentage of 2-hydroxyethyl methacrylate), and porogenic solvent 60 wt % (consisting of 32 (a), 45 (b), and 30 (c) wt % 1-dodecanol and complementary percentage of cyclohexanol); polymerization time, 16 h at room temperature.

moieties do not show appreciable differences in selectivities. The second factor is polymer morphology in the micropore range. It is well known[56] that changes in polymerization temperature vary the solvency of the system affecting the onset and rate of phase separation and thereby modifying the separation properties.

Effect of Cross-Linking. Yet another variable that affects the properties of monolithic materials is the percentage of cross-linking monomer in the polymerization mixture.[57,58] Its effects on the properties of the monoliths prepared in this study are rather complex. For example, the mode pore size of a material cross-linked with 16% EDMA in the polymerization mixture (40% of total monomers) using a 1:1 mixture of dodecanol and cyclohexanol as a porogenic solvent is close to 700 nm (Table 3). In contrast, the modal pore diameters of monoliths cross-linked with 8 and 4% EDMA in the reaction mixture (20 and 10% of total monomers) are significantly larger, reaching 1046 and 1097 nm, respectively. No pores could be detected for a material prepared with a cross-linker content of only 2% EDMA (5% of monomers) in the polymerization mixture, since this low percentage of cross-linker appears to be insufficient to enable phase separation and the creation of macroporosity under these conditions. The resulting monolith has a gellike character instead.

Decreases in cross-linking density lead to materials with both lower pore volumes and surface areas. Again, the "dry state" modal pore size can be adjusted by varying the dodecanol content in the polymerization mixture, thus obtaining materials with comparable porosity and different cross-linking levels. SEM micrographs of dry monoliths with equivalent porous properties (modal pore size 1162, 1046, and 1097 nm) and cross-linking levels of 40, 20, and 10% (related to total monomers) shown in Figure 6 do not reveal any significant differences. However, the less cross-linked monolithic columns exhibit better CEC performance. For example, the column efficiencies calculated from the separations of DNB-Leu enantiomers shown in Figure 7 increase from ~7000 plates/m using the 30% cross-linked monolith, to 36 000 plates/m for the 20% cross-linked material, to 74 000 plates/m for the 10% cross-linked monolithic CSP. The tradeoff for this rapid increase in efficiency is lower flow velocity resulting in longer run times. This effect can be explained by the swelling of the matrix. Although the pore sizes of these chiral monoliths as determined in the dry state are comparable (Table 3 and Figure 6), the less cross-linked materials swell to a larger extent. Since the volume within the capillary is fixed, swollen polymer partly fills the measured pore volume, and the actual pore size is smaller than that measured in the dry state. Unfortunately, current experimental methods do not allow accurate measurements of porous properties in the "operational" swollen state. [43] As a result of this

(57) Viklund, C.; Svec, F.; Fréchet, J. M. J.; Irgum, K. *Chem. Mater.* **1996**, *8*, 744−750.
(58) Viklund, C.; Pontén, E.; Glad, B.; Irgum, K.; Hörsted, P.; Svec, F. *Chem. Mater.* **1997**, *9*, 463−471.

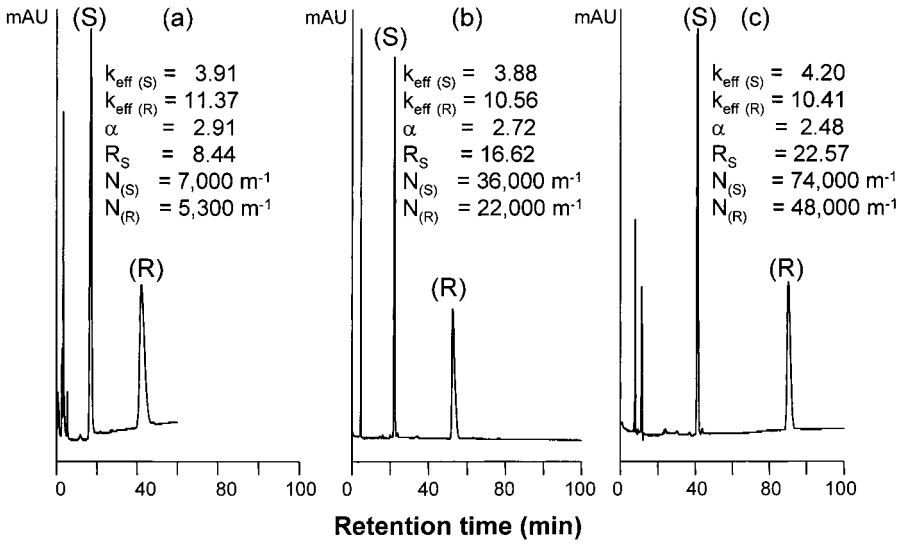

Figure 7. Effect of cross-linking on electrochromatographic separation of DNB-(*R*,*S*)-leucine. Conditions: capillary columns, 335 mm (250-mm active length) × 0.1 mm i.d. prepared by UV-initiated polymerization, pore size 1163 (a), 1265 (b), and 1097 nm (c); mobile phase, 0.4 mol/L acetic acid and 4 mmol/L triethylamine in acetonitrile/methanol (80:20, v/v); voltage, −25 kV; temperature, 50 °C; polymerization mixture, total monomers 40 wt % (consisting of chiral monomer 8 wt %, ethylene dimethacrylate 16 (a), 8 (b), and 4 wt % (c), complementary percentage of 2-hydroxyethyl methacrylate), and porogenic solvent 60 wt % (consisting of 32 (a), 45 (b), and 30 (c) wt % 1-dodecanol and complementary percentage of cyclohexanol); polymerization time, 16 h at room temperature.

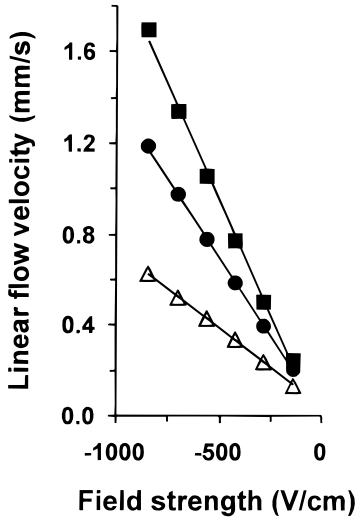

Figure 8. Effect of electric field strength on linear flow velocity for monolithic columns prepared with different percentage of cross-linking. Conditions: capillary columns, 335 mm (250-mm active length) × 0.1 mm i.d. prepared by UV-initiated polymerization, pore size 1163 (■), 1265 (●), and 1097 nm (△), acetone as EOF marker; mobile phase, 0.4 mol/L acetic acid and 4 mmol/L triethylamine in acetonitrile/methanol (80:20, v/v); temperature, 50 °C; polymerization mixture, total monomers 40 wt % (consisting of chiral monomer 8 wt %, ethylene dimethacrylate 16 (■), 8 (●), and 4 wt % (△), complementary percentage of 2-hydroxyethyl methacrylate), and porogenic solvent 60 wt % (consisting of 32 (■), 45 (●), and 30 (△) wt % 1-dodecanol and complementary percentage of cyclohexanol); polymerization time, 16 h at room temperature.

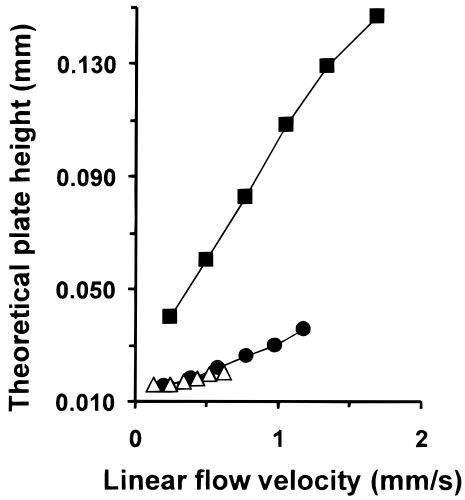

Figure 9. Effect of linear flow velocity on theoretical plate height for monolithic columns prepared with different percentage of cross-linking. Conditions: capillary columns, 335 mm (250-mm active length) × 0.1 mm i.d. prepared by UV-initiated polymerization; pore size, 1163 (■), 1265 (●), and 1097 nm (△), analyte, DNZ-(*S*)-leucine, acetone as EOF marker; mobile phase, 0.4 mol/L acetic acid and 4 mmol/L triethylamine in acetonitrile/methanol (80:20, v/v); temperature, 50 °C; polymerization mixture, total monomers 40 wt % (consisting of chiral monomer 8 wt %, ethylene dimethacrylate 16 (■), 8 (●), and 4 wt % (△), complementary percentage of 2-hydroxyethyl methacrylate), and porogenic solvent 60 wt % (consisting of 32 (■), 45 (●), and 30 (△) wt % 1-dodecanol and complementary percentage of cyclohexanol); polymerization time, 16 h at room temperature.

swelling, the slopes of the flow velocity versus field strength plots shown in Figure 8 are lower for the less cross-linked monoliths. This means that it is impossible to achieve a significant increase in EOF by changing the applied voltage.

The decrease in flow velocities has a positive effect on the efficiencies of all three monolithic columns, as confirmed by the van Deemter's theoretical plate height versus flow velocity plots (H/u curves) shown in Figure 9 for the separation of the DNZ-Leu enantiomers. The largest slope is observed for the most cross-linked monolith, indicating a significant contribution of the C term—related to the mass transport resistance within the separation medium—to peak dispersion. In contrast, the efficiencies of the 20 and 10% cross-linked monolithic columns appear to be

affected much less by flow velocity, although the limited range of flow velocities that can be achieved using acceptable field strengths does not allow generalization of this effect. Furthermore, the van Deemter's *A*-term contribution resulting from flow path nonuniformity that likely originates from inhomogeneities of the chromatographic bed appears to be lower for the less cross-linked monoliths, therefore affording much better efficiencies. None of the van Deemter plots reaches its minimum even at the lowest flow velocity obtained at −5 kV. This indicates that even higher efficiencies could theoretically be possible. However, the retention times required for such separations would be unacceptably long.

CONCLUSION

"Molded" monoliths prepared by the copolymerization of a solution of quinidine-derived monomer, a cross-linker, and a polar monomer in the presence of a porogenic solvent within the confines of untreated fused-silica capillaries are attractive separation media for chiral capillary electrochromatography. A major advantage of these monolithic capillary columns is their ease of preparation by a simple "molding" process that avoids the fabrication of frits and the packing of small beads into capillaries. Our results clearly demonstrate that a careful optimization of the material variables enables substantial improvements in both efficiency and selectivity of chiral CEC separations to be achieved. Further improvements in these separations are expected to result from the optimization of the chromatographic conditions, and these will be presented in the second part of this study.

ACKNOWLEDGMENT

Support of this research by a grant of the National Institute of General Medical Sciences, National Institutes of Health (GM-48364) and by the Division of Materials Sciences of the U.S. Department of Energy under Contract No. DE-AC03-76SF00098 is gratefully acknowledged. M.L. is grateful to the Max Kade Foundation for granting a research scholarship.

Received for review March 17, 2000. Accepted June 28, 2000.

AC000322L